Testing fiber tapers for use in the SDSS-V Focal Plane System

Sarah Tuttle[a,b], Emily Farr[a,b], Claire Poppett[c], Colby Jurgenson[d], José Sánchez-Gallego[a,b], Debra Fischer[e], Ryan Petersburg[e], Richard Pogge[b,d], and Juna Kollmeier[b,f]

[a]University of Washington, Seattle, Department of Astronomy, Seattle, WA, 98195
[b]Sloan Digital Sky Survey - V
[c]Space Sciences Laboratory, University of Berkeley, Berkeley, CA, 94720
[d]Ohio State University, Columbus, OH, 43210
[e]Yale University, New Haven, CT, 06520
[f]Carnegie Observatories, Pasadena, CA, 91101

ABSTRACT

We present measurements of 40 fiber tapers created as a possible approach to feed the BOSS spectrographs for SDSS-V in the Southern hemisphere at Las Campanas observatory. The fibers are designed with $180\mu m$ core at the input (telescope feed) end, and tapering to a $120\mu m$ core at the output (spectrograph) end. The taper is located in close proximity to the output end and is protected by metal strain relief held in place by the ferrule. We find the fiber tapers to provide adequate throughput but to underperform related to standard (untapered) fibers when it comes to FRD. We present here measurements from three different test bench setups, located at the University of Washington, Yale University, and SSL at the University of California, Berkeley. We find that although the overall throughput is high, the FRD is poor in the tapers. The current fiber taper performance is not adequate for the SDSS-V fiber requirements.

Keywords: optics, fiber optics, photonics, astronomical instruments

1. INTRODUCTION

The Sloan Digital Sky Survey V (SDSS-V) has begun early observations as of Fall of 2020. In preparation for SDSS-V, work was undertaken to support the evolution from SDSS-IV and SDSS-V. This work includes migration from a fiber plugging system to a focal plane system (FPS) populated with fiber positioning robots as well as an expansion to fully observe in the optical and infrared bandpasses in both the Northern and Southern Hemispheres with matching BOSS[1] and APOGEE[2] spectrographs. Of the three mapper projects, two (Black Hole Mapper and Milky Way Mapper) will use the FPS in both hemispheres to complete their surveys. The Northern site is the SDSS 2.5m telescope at Apache Point Observatory (APO), located in Sunspot, New Mexico.[3] In the South, SDSS observes with the 2.5m Dupont Telescope[4] at Las Campanas Observatory, in Chile. The expansion to the optical regime at LCO introduced potential challenges, as the telescope design is somewhat different and feeds the fibers at a slower speed than the current system. We present here work to investigate fiber tapers as a way to mitigate differences in the two observational setups. APO currently feeds $120\mu m$ core fibers, and initial estimates proposed that $180\mu m$ core fibers would provide an optimal match with the APO/BOSS performance.

1.1 Fiber Optics in Astronomy

Fiber optics used for astronomical instruments have evolved considerably since they were first considered in the late 1970s.[5] Improvements in manufacturing have greatly increased their throughput as well as the bandpass over which they transmit adequately for astrophysical observations. Fibers were initially used in the red and infrared bands, where longer wavelengths assisted in limited scattering losses. As fiber draws have become more consistent and materials have become less contaminated, blue and ultraviolet performance has improved. Initially used as static fibers and bundles (PPak,[6,7] Sparsepak,[8,9] FIREBall,[10] MANGA[11]), fibers have now been deployed

Further author information: Send correspondence to S. Tuttle: E-mail: tuttlese@uw.edu

regularly in systems with large and small ranges of motion (HYDRA,[12] Starbugs,[13] MOONS,[14,15]VIRUS,[16,17] PFS[18]). These fibers have all been standard circular fibers. Recent photonics work has pushed into novel fibers, including octagonal fibers (used to improve scrambling,[19] although ongoing studies are revealing more about different sources of noise[20]), and fiber shaping such as fiber tapers and multi-core fibers.[21] We hope by testing across several platforms we clearly constrain performance and provide connection to past measurements (and measurements on different styles of test bench).

1.2 Characterizing Fiber Optics

The fundamental parameters that impact performance for astronomical applications are the focal ratio degradation (FRD) and the throughput as a function of wavelength.

FRD has a variety of causes that have been characterized throughout the last several decades. Early work to understand fibers noted that large scale motion or bending did not have a strong impact on fiber FRD, while identifying buffer size and hardness as well as input ratio as having some impact.[22] More recent work has shown termination technique can have a strong impact on the FRD of a fiber and suggests in situations where it is feasible, cleaving fibers preserves their optical performance.[23] As instrumentalists working with fiber have become more comfortable with it, techniques have been developed to understand the components of FRD to allow for the removal of their effects as instruments are designed and data is taken.[24]

1.3 Fibers in SDSS-V

SDSS spectroscopy and fibers have gone hand in hand since the earliest days of SDSS. Since the start of SDSS fiber spectroscopy, plug plates have been deployed. The aluminum plates are drilled at the University of Washington, delivered to the observatories, and then hand plugged in specially built cartridges that are installed and changed throughout the night's observations. Each plate matches one pointing, and when a pointing has been adequately observed the plate is retired. The cartridges are reused and replugged as new plates are observed.

SDSS-V is changing the approach to fiber spectroscopy to increase the observing efficiency and greatly increase the size of the survey. SDSS has long focused on improving systems to maximize the overall observational system efficiency, and had reached the limit of improving the current process. Each generation of SDSS has examined the current system to consider potential upgrades and technical improvements that could be adopted.

At this transition from SDSS-IV to SDSS-V, the decision has been made to move from manually plugged plates to fiber positioning robots. This approach has been considered before but now has reached a state of technical feasibility where the technical gains balance the risks. This requires a significant infrastructure upgrade in both hemispheres to build and install the focal plane system (FPS). Built to interface in a similar way to the hand-plugged cartridges, the FPS is a (relatively) permanently installed "cartridge" that carries 500 fiber robots. Each robot has the capacity to carry an APOGEE (IR) fiber, a BOSS (optical) fiber, and a metrology fiber for a back illumination system.

As mentioned earlier, the Northern and Southern telescopes are a different optical design. Before beginning the final FPS fiber work, we undertook an investigation of fiber tapers as a possible option to improve throughput from the LCO-based Dupont telescope to the newly relocated BOSS spectrograph.

1.4 This paper

This paper will start by describing the fiber tapers used in the experiments. We will then go on to describe and compare the three fiber measurement setups used in Section 3. In Section 4 we present and compare the measurements across the different setups and in Section 5 we discuss the path forward for SDSS-V and future possibilities with fiber tapers.

2. TAPER SPECIFICATIONS

The tapers measured here all come from a set of 40 tapers ordered from Ceramoptec, received in August of 2019. The tapers were terminated at UW on the $180 \mu m$ end before they were measured and distributed to the other two test sites for comparison. The $120 \mu m$ end was terminated with a stainless steel ST connector by Ceramoptec prior to shipment, in order to connectorize and add the metal stabilizing sheath over the taper joint at the same time. The taper joint is located near the ST connector.

2.1 Ceramoptec Fiber Tapers

The Ceramoptec tapers are 180/216/240 fibers that were drawn down to the 120μm core with a 144μm cladding. The tapering was done close to one of the connectorized ends rather than happening centrally. The test batch tapers were made contemporaneously.

3. FIBER TAPER MEASUREMENTS

3.1 UW Experimental Setup

The optical test bench that was developed at the University of Wisconsin for SDSS-III and SDSS-IV was used for the testing of the fiber tapers. This allowed us to compare earlier fiber optic harnesses from BOSS against the tapers performance using reference fibers (which were measured regularly and also sent to the two remote test sites). The test stand was originally designed to allow testing at f/5 only, which is the input of the Sloan 2.5 meter at Apache Point Observatory. Prior to starting taper testing, the test stand was adapted to allow for an additional f/7.5 input, which allowed us to test for the Irénée Dupont telescope at Las Campanas Observatory.

Each taper was tested at both F ratios and with two colored glass bandpass filters, BG-38 (CW 470nm, FWHM 271nm) and Hoya RT-830 (CW 830nm, FWHM 260 nm) resulting in 4 measurements for each fiber.

The light source on the SDSS test bench is a Newport 780 Tungsten Halogen Lamp(50W) white light set to 80 percent intensity. From the output of the lightsource, a pellicle beamsplitter then sends light to the input camera, a monochrome Manta G-201B camera (4.4 m X 4.4 m pixel size and an ASG protective coating) and through an achromatic Rolyn 5:1 microscope objective to the output camera. The input and output cameras are identical. The fiber is then centered on the beam with the use of the input camera and manual operator checks. The output camera exposure is set in accordance with the filter in use. In this case, exposure times were 1 ms for the BG-38 filter and 4ms for the RT-830 filter.

Measurements of a standard BOSS fiber, with no taper, gave us a range of expected performance. The throughput at f/3.2 for a fiber that is performing optimally should fall within 90 % $\pm$ 3%.

The optical test bench takes measurements of relative FRD and throughput at certain f ratios. A measurement is made by initially taking an image of the source. The program then measures the apertures of the source light before moving to take an image of the fiber, now illuminated with by the source. The program then finds the throughput at f/3.2, f/4 and f/5 and compares it to the same f ratios measured on the source light. Finally, a second image is taken of the source and checked against the original to ensure that the change in flux between the two source images is less than 0.5 percent.

3.2 SSL Experimental Setup and Procedure

The SSL setup is shown in diagram form in Figure 1, and laid out on the optical bench in Figure 2. It is designed to use an obscuration and feeds at f/4 to mimic the Keck telescope illumination. The testing was done on-axis with a 530nm LED fed by a 50μm pupil centered on the fiber and aligned with the optical axis of the fiber.

First, the output CCD camera is moved to the location of the fiber input, and a far-field image is recorded to calibrate the throughput. Then the setup is returned to the nominal configuration (seen in Figure 2). The BOSS reference fiber is placed in the test setup and aligned with respect to all three axes using the input spot alignment camera. The "extreme" aperture mask is installed and the fiber is aligned in tip/tilt. This is cycled until the tip, tilt, and x/y/z position are centered. An image is taken with the output CCD, and then the camera is moved back 5mm and another image is taken. The LED is switched off, and the background image is taken. The reference fiber is removed, and the same process is executed with each fiber taper (the 180μm as the input, and the tapered end as the output). The test cycle is closed out with a final set of measurements on the reference fiber.

3.3 Yale Experimental Setup

The Yale Fiber Characterization Station (FCS) was built by Ryan Petersburg for testing and development of the fibers and scrambling mechanisms for the precision RV planet hunter, EXPIRES, recently commissioned on the Discovery Channel Telescope.[25] This setup is shown in Figure 3 and Figure 4.

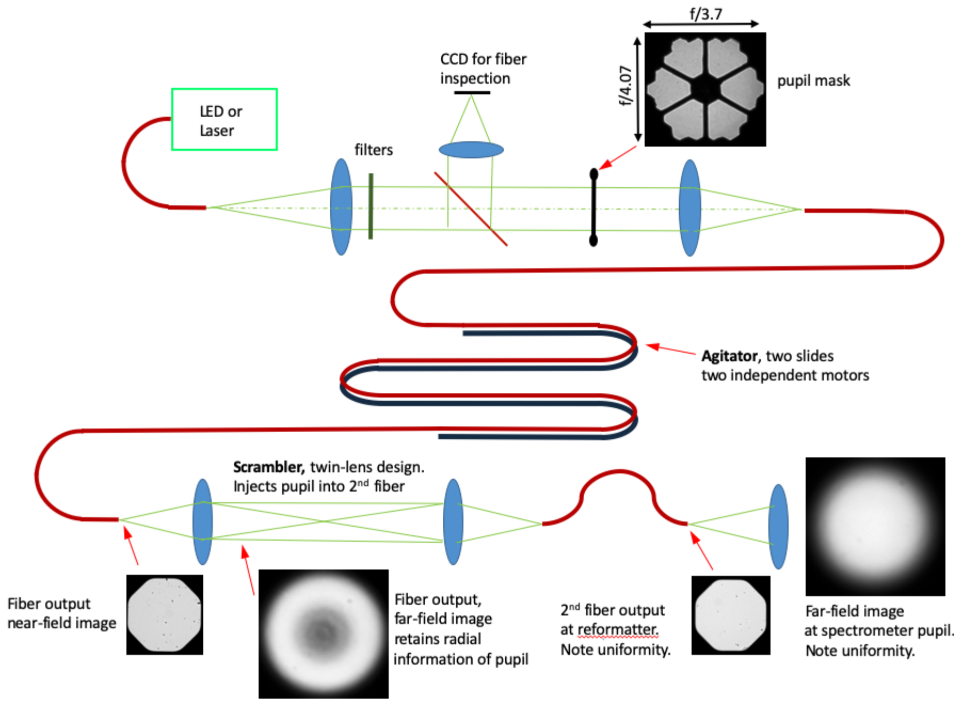

Figure 1. Diagram of the SSL experimental setup.

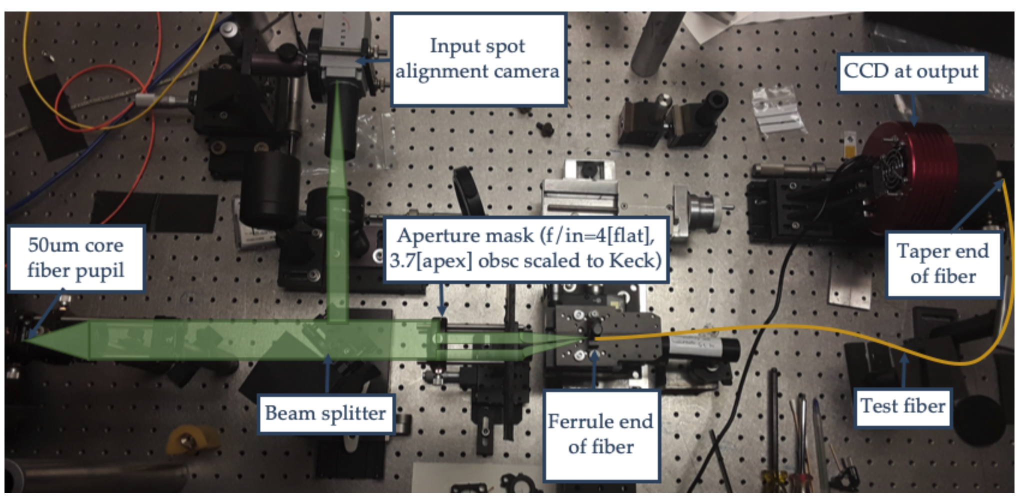

Figure 2. Photograph of the SSL experimental setup.

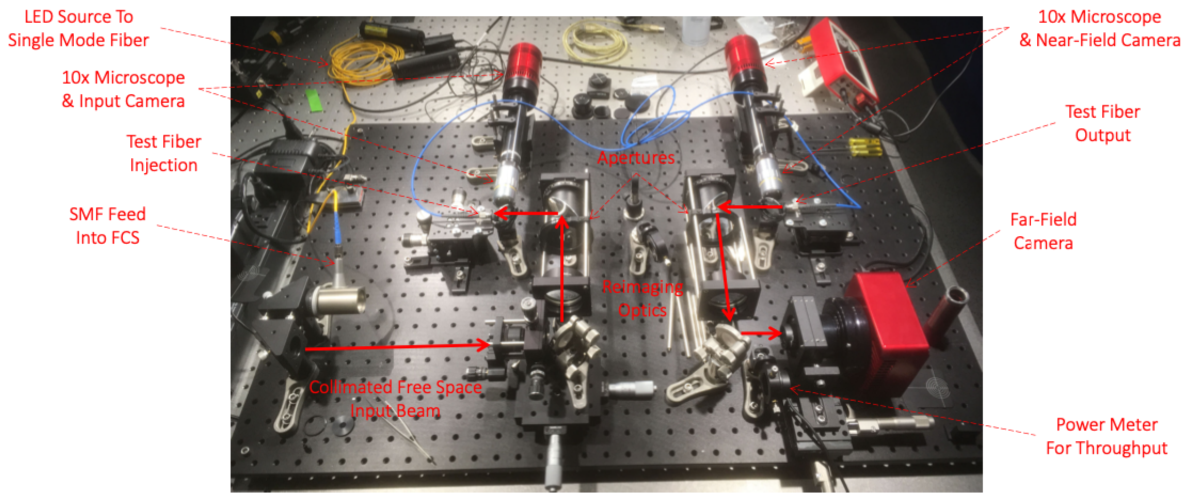

Figure 3. Yale FCS configured to measure FRD.

3.3.1 FRD Experimental Setup and Procedure

The setups used for the FRD and throughput tests were slightly different, as shown in the two figures. For the FRD measurements, the input sources were two LEDs at 455nm and 625nm, each with a 30nm bandwidth. For each fiber, the following procedure was followed. First, a series of 10 dark and ambient exposures are taken at the same exposure time as the far-field images. Then, the aperture in the fiber injection arm is set to completely fill the numerical aperture of the fiber and the beam is centered on the core. A series of 10 far-field exposures are taken with the output arm aperture set at f/3, f/4, and f/5. These measurements are used as the FRD baseline. The aperture then is set to f/5. A series of 10 far-field exposures are taken with the output aperture completely open. The apeture is set to f/7.5. A final series of 10 far-field exposures are taken with the output aperture completely open.

3.4 Throughput Experimental Setup and Procedure

The throughput measurements are made using a 635nm laser. Measurements are made at two input apertures, f/5 and f/7.5. The output aperture was completely open to capture all exiting light. To measure throughput, the beam is first aligned to the fiber core (as is done with the FRD measurements), then the pellicle beamsplitters are removed from the beam path. The power meter located in front of the far-field camera is moved into the beam. The total throughput (of the optics plus the fiber) is measured (in watts). The OAPs (off-axis parabolic mirrors) at the input and output of the fibers are rotated 180° to face each other so the that the beam path bypasses the fiber (seen as the yellow arrow in Figure 4.) The throughput of the optics is measured in watts. The throughput of the fiber is calculated as a ratio of the two previous measurements.

4. RESULTS

Although the test setups vary in several details (including the kind of input light and measurement technique) we see similar results across the test setups. We also find the BOSS reference fibers used to connect the measurement setup perform as expected, increasing our confidence in the results across platforms.

4.1 Data

Here we present the data from each of the test setups separately. This allows comparison between fibers measured on each setup. The setups have been built to model different telescope systems, so we wait until Section 4.2 to make comparisons between the measurements.

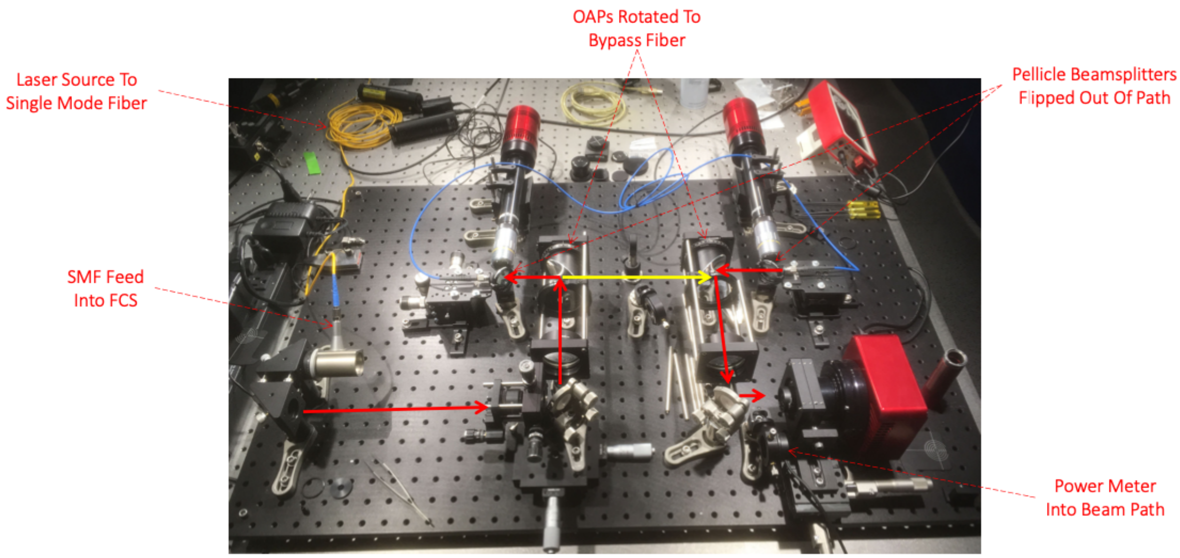

Figure 4. Yale FCS configured to measure throughput.

4.1.1 UW Test Stand Data

Each fiber taper was initially measured twice in the UW test stand. Between all measurements (including of the same fiber) tapers were removed and re-mounted to ensure there were no mounting or placement issues. Three separate references fibers, made with fiber used on the BOSS Spectrograph, were measured with each change of input f ratio and filter. Reference fiber 1 was kept at UW, reference fiber 2 was sent to Yale and reference fiber 3 was sent to SSL. A summary of results from these measurements can be seen in Table 1. It is clear from the average measurements that the performance across the collection of tapers is quite variable. As can be seen from the table, the reference fibers were quite stable even though they were both handled more and measured more frequently than the fiber tapers. The wide variation in the fiber tapers is seen across measurement wavelength and f-number, with the most variation seen at the smaller f-number.

Once the initial measurements were completed, ten tapers were sent to SSL, and ten were sent to Yale for measurement.

4.1.2 SSL Test Stand Data

Table 3 shows fiber tapers 11-20, as measured on the SSL Test Stand. The reference fiber shows output as expected from a standard untapered BOSS fiber. The fiber tapers perform as expected - overall the total throughput is similar to the reference fiber, except for two exceptions (referred to as T11 and T19).

4.1.3 Yale Test Stand Data

Data from the Yale FCS was used to measure several key characteristics of the fibers, including the encircled energy as a function of input beam and illumination wavelength, throughput, and a comparison of the input to output F-ratios. In Figure 5 we show the encircled energy measured with two different input wavelengths (455nm, in the left column and 625nm, in the right column) as well as two different input f-numbers, with the top row input illumination at f/5.0 and the bottom row input at f/7.5.

Figure 6 shows the input versus output f-ratios of the ten tapered fibers measured at Yale. For both plots the ideal taper performance is marked with a black dashed line. The fiber taper performance is shown by the solid colored dashes and lines. We compare the two input illuminations and don't see a strong variation. The output f-ratio is being altered in most cases, but much less strongly than the ideal case.

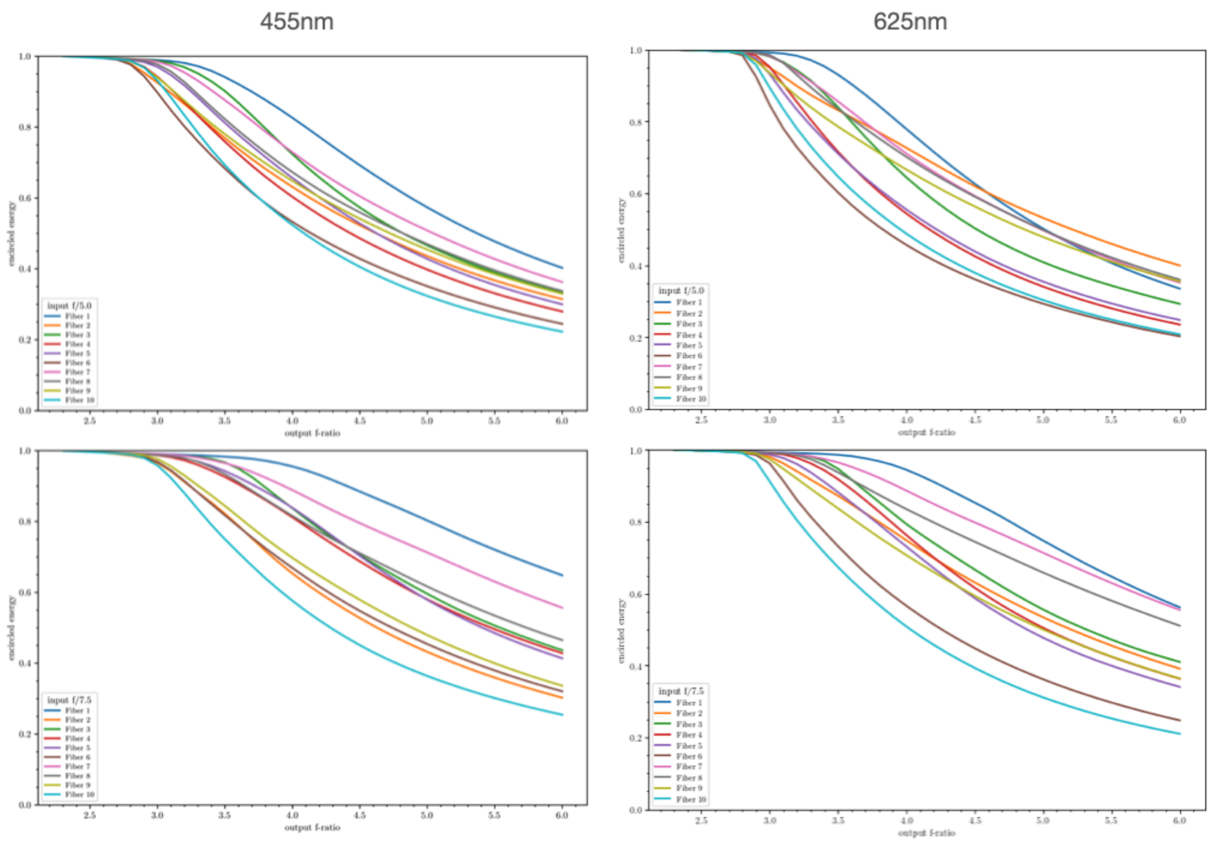

Figure 5. Encircled energy shown as a function of input illumination wavelength and f-number from Yale setup.

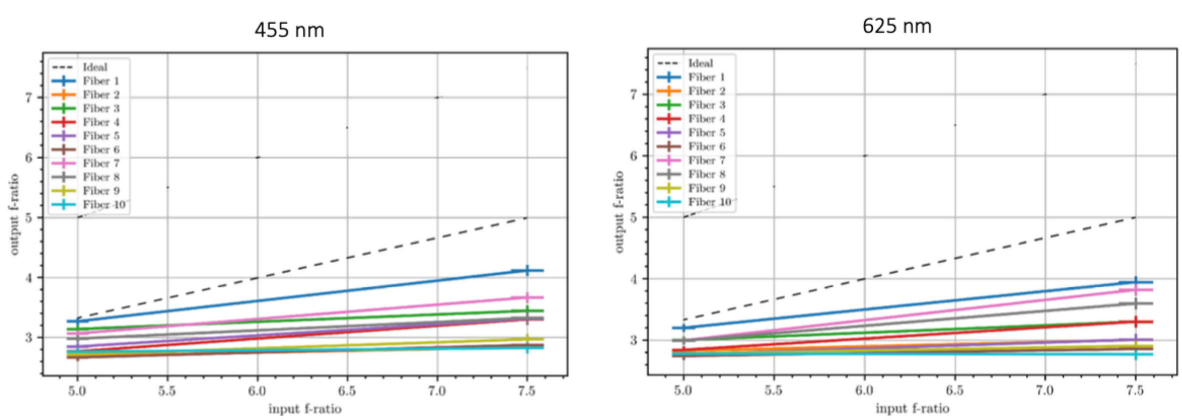

Figure 6. Input to Output F-Ratio from Yale FCS.

Table 1. UW test stand average throughput for all tapers

Taper	% within f/3.2	% within f/4	% within f/5
Ref	90.7 ± 1.5	90.2 ± 1.5	89.5 ± 1.5
1	87.33 ± 6.01	71.15 ± 8.02	54.94 ± 9.83
2	61.68 ± 6.5	46.92 ± 5.37	36.03 ± 5.01
3	74.05 ± 11.43	54.59 ± 9.71	39.92 ± 6.31
4	70.85 ± 7.83	54.6 ± 9.7	39.93 ± 6.31
5	72.1 ± 11.43	53.17 ± 11.7	38.37 ± 8.6
6	55.52 ± 14.8	40.41 ± 12.93	29.52 ± 10.29
7	78.18 ± 5.17	60.28 ± 4.02	45.64 ± 3.3
8	57.38 ± 10.59	42.10 ± 9.06	31.40 ± 7.93
9	68.55 ± 11.17	52.80 ± 10.32	40.37 ± 8.50
10	51.82 ± 12.51	35.87 ± 9	25.17 ± 6.42
11	74.05 ± 9.14	56.24 ± 7.72	41.51 ± 6.16
12	60.99 ± 7.4	44.56 ± 6.55	31.79 ± 4.92
13	67.14 ± 11.09	47.91 ± 9.88	34.29 ± 8.34
14	44.83 ± 9.42	32.53 ± 8.11	23.98 ± 6.74
15	59.94 ± 11.29	43.17 ± 9.3	30.73 ± 7.01
16	55.68 ± 8.76	40.42 ± 8.08	29 ± 6.32
17	49.48 ± 4.62	36.13 ± 4.59	26.41 ± 4.76
18	61.29 ± 2.54	45.72 ± 2.60	33.98 ± 2.57
19	41.89 ± 13.30	29.82 ± 11.58	21.27 ± 9.02
20	68.72 ± 8	52.‘5 ± 8.03	38.92 ± 7.55
21	59.49 ± 6.59	44.60 ± 5	33.75 ± 3.88
22	68.42 ± 4.22	50.49 ± 2.26	37.52 ± 1.28
23	70.84 ± 6.80	52.64 ± 6.23	38.48 ± 4.54
24	64.17 ± 6.81	46.54 ± 5.23	33.66 ± 3.70
25	55.69 ± 9.50	41.47 ± 8.85	30.45 ± 7.33
26	48.87 ± 8.93	35.02 ± 7.36	25.53 ± 6.22
27	52.96 ± 9.35	37.82 ± 7.13	27.96 ± 5.84
28	71.34 ± 8.13	53.88 ± 6.69	40.50 ± 5.82

4.2 Data Comparison

Here we compare data from setup to setup to better understand the root causes of the fiber taper behavior. One key result to note - the SSL and Yale setups measures total throughput. When one doesn't constrain the radius of the output light, the majority of the light can be recaptured at the output end. Unfortunately, if light like this were injected into a spectrograph it would severely degrade spectrograph performance.

4.3 Far Field Image Examples

We find the far field images to be particularly insightful in gaining a more physical intuition about the results reported above. Figure 7 shows a series of images from the Yale FCS to demonstrate the range of behaviors in

Table 2. UW test stand average throughput for all tapers cont.

29	65.68 ± 3.34	47.36 ± 2.40	34.58 ± 2.3
30	53.74 ± 4.44	39.19 ± 3.96	28.65 ± 3.63
31	74.29 ± 5.47	53.89 ± 3.04	38.97 ± 1.75
32	45.79 ± 13.61	32.63 ± 12.09	24.06 ± 10.29
33	66.44 ± 8.71	47.34 ± 5.35	34.03 ± 4.67
34	75.94 ± 6.36	55.88 ± 3.38	41.34 ± 2.02
35	55.96 ± 8.07	39.92 ± 7.07	28.78 ± 5.24
36	65.08 ± 13.09	48.13 ± 10.26	35.59 ± 7.54
37	60.47 ± 13.54	42.50 ± 8.37	30.08 ± 5.52
38	62.98 ± 13.22	45.99 ± 11.02	32.91 ± 8.12
39	60.14 ± 3.85	45.76 ± 2.97	34.22 ± 1.93
40	47.46 ± 3.06	33.75 ± 3.12	24.64 ± 3.11
PolyMicro	54.5 ± 12.7	39.6 ± 9.3	30.1 ± 7.1

Table 3. Encircled Energy from SSL Test Stand

	EE within 90%	EE within 95%	EE within 97%	% of output
Ref	4.05	3.86	3.74	85.55
T11	2.63	2.48	2.43	38.36
T12	2.69	2.56	2.48	85.47
T13	2.79	2.63	2.55	86.31
T14	2.75	2.63	2.56	84.88
T15	2.70	2.56	2.50	85.36
T16	2.58	2.41	2.33	78.36
T17	2.81	2.67	2.61	84.14
T18	2.61	2.47	2.39	82.04
T19	2.94	2.80	2.83	31.23
T20	2.71	2.57	2.50	81.07
Ref	4.10	3.85	3.67	86.59

the fiber tapers. One of the issues that clearly must be resolved before these sorts of fibers can deployed in more standard instruments is less variable behavior.

We show comparisons between the best case fiber (Fiber 1) measured at Yale on the left, and the worst case fiber (Fiber 6) on the right. The left hand column has a f/5 input, and the right hand column has an f/7.5 input. The left four images are taken with 455nm illumination, and the right four images measured with 625nm illumination.

Similar results are seen from the far-field images taken with the SSL setup, as seen in Figure 8. We again see the very clear ring structure, and the low light level at the core of the fibers. These geometric structures are extremely different from what you see in a standard fiber, which may show some variation across the illuminated surface but should not show the deep structural differences we see here.

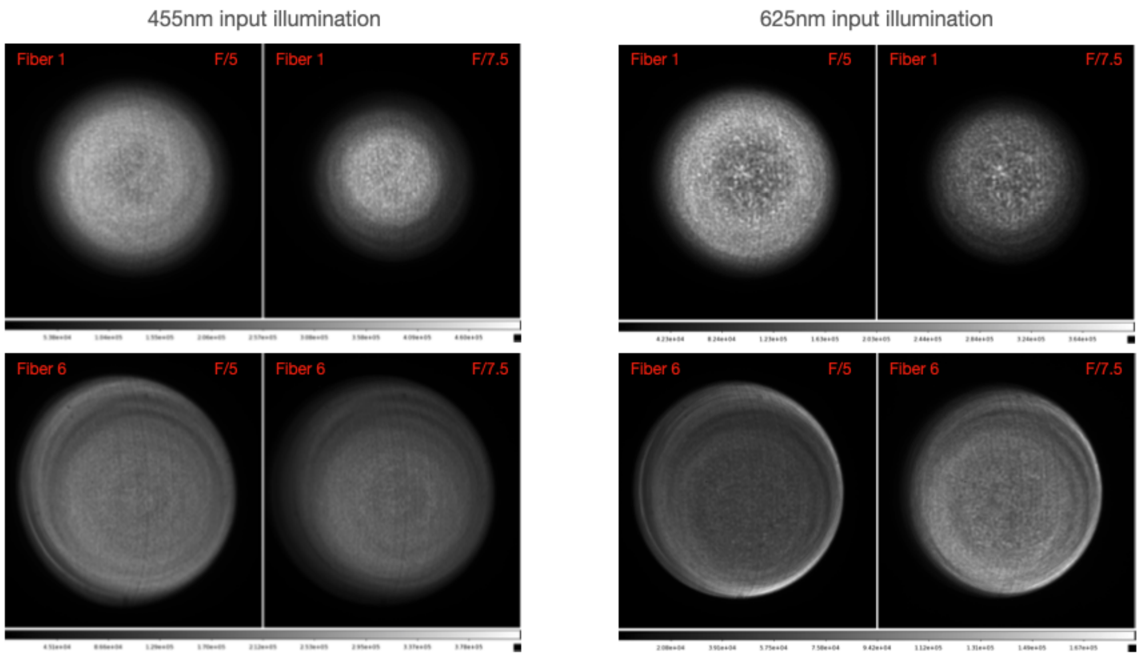

Figure 7. Far-field fiber images from Yale FCS.

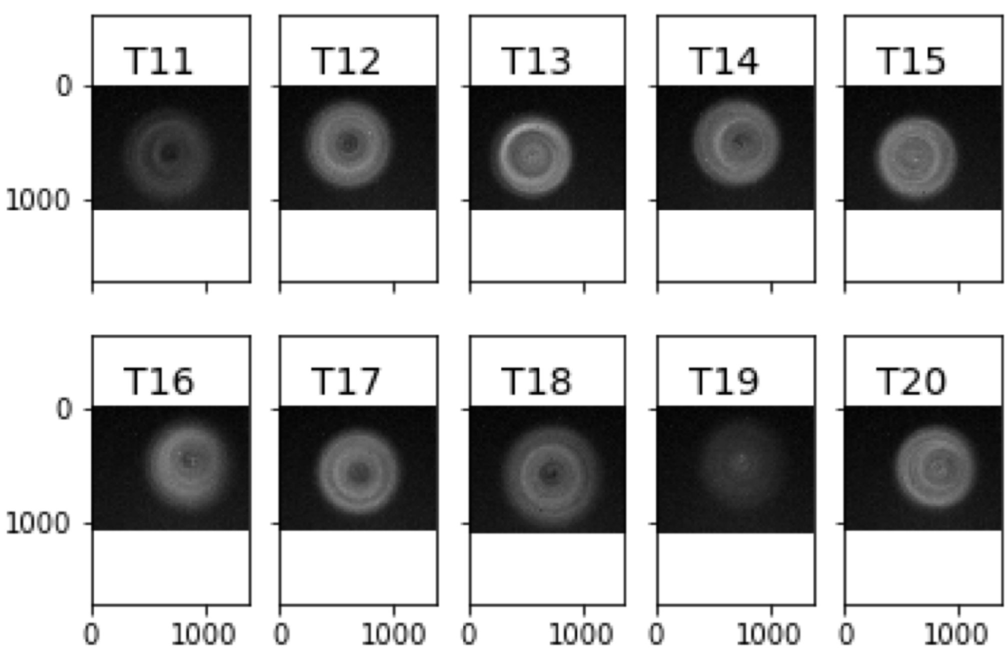

Figure 8. Far-field fiber images from all 10 SSL measured fibers.

Table 4. Throughput characteristics for f/5 and f/7.5 input beams from Yale FCS.

	f/5	f/7.5
Median	0.827	0.776
Standard Dev	0.039	0.042
Minimum	0.741	0.693
Maximum	0.868	0.825

5. CONCLUSIONS

The results show overall throughput to be high, but the FRD to be unacceptable. We believe this shows that the light isn't being lost during the travel through the fiber, but the method of the taper is inducing stress that is throwing light preferentially out of the core of the fiber. We note behavior that is especially problematic for fibers used in astronomical instruments. The fibers were found to frequently have variable performance from measurement to measurement, even on the same setup. We suspect this lack of repeatability comes from the unstable nature of the induced stress at the taper, but at this time that is only speculation. Standard untapered fibers have been shown to be relatively stable through long term motion of different scales, and especially with the trend towards fiber positioners this behavior of fiber tapers should be further investigated before they are deployed.

Performance of currently available commercial fiber tapers are not adequate for the task investigated. The data looks suspiciously like induced stress, which leads the authors to believe this problem could likely be addressed during manufacturing of the tapers. However, for the SDSS-V application investigated, fiber tapers are not adequate and will not be applied.

Disclosures

The authors have no relevant financial interests or conflicts.

ACKNOWLEDGMENTS

Funding for the Sloan Digital Sky Survey V has been provided by the Alfred P. Sloan Foundation, the Heising-Simons Foundation, and the Participating Institutions. SDSS acknowledges support and resources from the Center for High-Performance Computing at the University of Utah. The SDSS web site is www.sdss5.org.

SDSS is managed by the Astrophysical Research Consortium for the Participating Institutions of the SDSS Collaboration, including the Carnegie Institution for Science, Chilean National Time Allocation Committee (CN-TAC) ratified researchers, the Gotham Participation Group, Harvard University, The Johns Hopkins University, L'Ecole polytechnique fédérale de Lausanne (EPFL), Leibniz-Institut für Astrophysik Potsdam (AIP), Max-Planck-Institut für Astronomie (MPIA Heidelberg), Max-Planck-Institut für Extraterrestrische Physik (MPE), Nanjing University, National Astronomical Observatories of China (NAOC), New Mexico State University, The Ohio State University, Pennsylvania State University, Smithsonian Astrophysical Observatory, Space Telescope Science Institute (STScI), the Stellar Astrophysics Participation Group, Universidad Nacional Autónoma de México, University of Arizona, University of Colorado Boulder, University of Illinois at Urbana-Champaign, University of Toronto, University of Utah, University of Virginia, and Yale University.

REFERENCES

[1] S. A. Smee, J. E. Gunn, A. Uomoto, *et al.*, "The Multi-object, Fiber-fed Spectrographs for the Sloan Digital Sky Survey and the Baryon Oscillation Spectroscopic Survey," *The Astronomical Journal* **146**, 32 (2013).

[2] J. C. Wilson, F. Hearty, M. F. Skrutskie, *et al.*, "The Apache Point Observatory Galactic Evolution Experiment (APOGEE) high-resolution near-infrared multi-object fiber spectrograph," in *Ground-based and Airborne Instrumentation for Astronomy III*, I. S. McLean, S. K. Ramsay, and H. Takami, Eds., *Society of Photo-Optical Instrumentation Engineers (SPIE) Conference Series* **7735**, 77351C (2010).

[3] J. E. Gunn, W. A. Siegmund, E. J. Mannery, *et al.*, "The 2.5 m Telescope of the Sloan Digital Sky Survey," *The Astronomical Journal* **131**, 2332–2359 (2006).

[4] I. S. Bowen and J. Vaughan, A. H., "The optical design of the 40-in. telescope and of the Irénée DuPont telescope at Las Campanas Observatory, Chile.," *Applied Optics* **12**, 1430–1434 (1973).

[5] J. R. P. Angel, M. T. Adams, T. A. Boroson, *et al.*, "A very large optical telescope array linked with fused silica fibers.," *The Astrophysical Journal* **218**, 776–782 (1977).

[6] M. A. W. Verheijen, M. A. Bershady, D. R. Andersen, *et al.*, "The Disk Mass project; science case for a new PMAS IFU module," *Astronomische Nachrichten* **325**, 151–154 (2004).

[7] A. Kelz, M. A. W. Verheijen, M. M. Roth, *et al.*, "PMAS: The Potsdam Multi-Aperture Spectrophotometer. II. The Wide Integral Field Unit PPak," *Proceedings of the Astronomical Society of the Pacific* **118**, 129–145 (2006).

[8] M. A. Bershady, D. R. Andersen, J. Harker, *et al.*, "SparsePak: A Formatted Fiber Field Unit for the WIYN Telescope Bench Spectrograph. I. Design, Construction, and Calibration," *Proceedings of the Astronomical Society of the Pacific* **116**, 565–590 (2004).

[9] M. A. Bershady, D. R. Andersen, M. A. W. Verheijen, *et al.*, "SparsePak: A Formatted Fiber Field Unit for The WIYN Telescope Bench Spectrograph. II. On-Sky Performance," *Astrophysical Journal Supplement* **156**, 311–344 (2005).

[10] S. E. Tuttle, D. Schiminovich, R. Grange, *et al.*, "FIREBALL: the first ultraviolet fiber fed spectrograph," in *Space Telescopes and Instrumentation 2010: Ultraviolet to Gamma Ray*, M. Arnaud, S. S. Murray, and T. Takahashi, Eds., *Society of Photo-Optical Instrumentation Engineers (SPIE) Conference Series* **7732**, 773227 (2010).

[11] N. Drory, N. MacDonald, M. A. Bershady, *et al.*, "The MaNGA Integral Field Unit Fiber Feed System for the Sloan 2.5 m Telescope," *The Astronomical Journal* **149**, 77 (2015).

[12] S. C. Barden and A. C. Rudeen, "Kitt Peak National Observatory fiber actuator device," in *Instrumentation in Astronomy VII*, D. L. Crawford, Ed., *Society of Photo-Optical Instrumentation Engineers (SPIE) Conference Series* **1235**, 729–735 (1990).

[13] J. Gilbert, M. Goodwin, J. Heijmans, *et al.*, "Starbugs: all-singing, all-dancing fibre positioning robots," in *Modern Technologies in Space- and Ground-based Telescopes and Instrumentation II*, R. Navarro, C. R. Cunningham, and E. Prieto, Eds., *Society of Photo-Optical Instrumentation Engineers (SPIE) Conference Series* **8450**, 84501A (2012).

[14] I. Guinouard, D. Lee, H. Schnetler, *et al.*, "Development of the fibres of MOONS," in *Advances in Optical and Mechanical Technologies for Telescopes and Instrumentation*, R. Navarro, C. R. Cunningham, and A. A. Barto, Eds., *Society of Photo-Optical Instrumentation Engineers (SPIE) Conference Series* **9151**, 91514S (2014).

[15] M. Cirasuolo and t. M. consortium, "MOONS: The New Multi-Object Spectrograph for the VLT," *arXiv e-prints* , arXiv:2009.00628 (2020).

[16] J. D. Murphy, G. J. Hill, P. J. MacQueen, *et al.*, "The influence of motion and stress on optical fibers," in *Ground-based and Airborne Instrumentation for Astronomy IV*, I. S. McLean, S. K. Ramsay, and H. Takami, Eds., *Society of Photo-Optical Instrumentation Engineers (SPIE) Conference Series* **8446**, 84465F (2012).

[17] A. Kelz, T. Jahn, D. Haynes, *et al.*, "VIRUS: assembly, testing and performance of 33,000 fibres for HETDEX," in *Ground-based and Airborne Instrumentation for Astronomy V*, S. K. Ramsay, I. S. McLean, and H. Takami, Eds., *Society of Photo-Optical Instrumentation Engineers (SPIE) Conference Series* **9147**, 914775 (2014).

[18] H. Sugai, H. Karoji, N. Takato, *et al.*, "Prime focus spectrograph: Subaru's future," in *Ground-based and Airborne Instrumentation for Astronomy IV*, I. S. McLean, S. K. Ramsay, and H. Takami, Eds., *Society of Photo-Optical Instrumentation Engineers (SPIE) Conference Series* **8446**, 84460Y (2012).

[19] G. Avila, "FRD and scrambling properties of recent non-circular fibres," in *Ground-based and Airborne Instrumentation for Astronomy IV*, I. S. McLean, S. K. Ramsay, and H. Takami, Eds., *Society of Photo-Optical Instrumentation Engineers (SPIE) Conference Series* **8446**, 84469L (2012).

[20] E. Oliva, M. Rainer, A. Tozzi, *et al.*, "Experimental characterization of modal noise in multimode fibers for astronomical spectrometers," *Astronomy & Astrophysics* **632**, A21 (2019).

[21] D. M. Haynes, I. Gris-Sanchez, T. A. Birks, *et al.*, "Optical fiber modal noise suppression in the NIR region using multicore fiber and photonic lanterns," in *Advances in Optical and Mechanical Technologies for Telescopes and Instrumentation III*, R. Navarro and R. Geyl, Eds., *Society of Photo-Optical Instrumentation Engineers (SPIE) Conference Series* **10706**, 1070665 (2018).

[22] L. W. Ramsey, "Focal ratio degradation in optical fibers of astronomical interest.," in *Fiber Optics in Astronomy*, S. C. Barden, Ed., *Astronomical Society of the Pacific Conference Series* **3**, 26–39 (1988).

[23] C. Poppett and J. Allington-Smith, "A new method to quantitatively compare focal ratio degradation due to different end termination techniques," in *Ground-based and Airborne Instrumentation for Astronomy III*, I. S. McLean, S. K. Ramsay, and H. Takami, Eds., *Society of Photo-Optical Instrumentation Engineers (SPIE) Conference Series* **7735**, 77350U (2010).

[24] D. M. Haynes, M. J. Withford, J. M. Dawes, *et al.*, "Focal ratio degradation: a new perspective," in *Advanced Optical and Mechanical Technologies in Telescopes and Instrumentation*, E. Atad-Ettedgui and D. Lemke, Eds., *Society of Photo-Optical Instrumentation Engineers (SPIE) Conference Series* **7018**, 70182U (2008).

[25] R. R. Petersburg, T. M. McCracken, D. Eggerman, *et al.*, "Modal Noise Mitigation through Fiber Agitation for Fiber-fed Radial Velocity Spectrographs," *The Astrophysical Journal* **853**, 181 (2018).